Available online at www.sciencedirect.com
ScienceDirect
Energy Reports 6 (2020) 43–52
www.elsevier.com/locate/egyr

4th Annual CDT Conference in Energy Storage and Its Applications, Professor Andrew Cruden, 2019, 07-19, University of Southampton, U.K.

Laboratory-based examination of the effect of rotational inertia on energy recuperation in the regenerative braking process

Adnan Alamili[a,b,*], Yiqin Xue[a], Fatih Anayi[a]

[a] *School of Engineering, Cardiff University, CF243AA, UK*
[b] *Department of Electrical Engineering, Faculty of Engineering, University of Kufa, P.O. Box (21), Iraq*

Received 13 February 2020; accepted 25 February 2020
Available online 6 April 2020

Abstract

Dynamic energy recovery in electric and hybrid electric vehicles can assist in restoring kinetic energy during descending and braking operations. The recouped energy can be stored in various storage units, such as a flywheel energy storage (FES) units, ultra-capacitors (UCs) or batteries, thus conserving energy for later use during acceleration condition. The FES is used in a variety of modern applications; for instance, it tends to be associated with the motor shaft to assist in starting the vehicle from rest. Several different components have been utilized to execute the motoring and braking mechanism in a structured test rig. However, there is an urgent need to represent this application within the limits of the laboratory facilities while being able to simulate the natural system. Consequently, this paper will examine the effect of rotating inertia at a different rotating speed in the drive system on propelled energy. It will also evaluate the stored energy in the UC storage unit and the braking time in the regenerative braking (RB) process. Moreover, it will demonstrate the experimental probing and mathematical modeling of the motor/flywheel (lumped into an equivalent inertial mass), which is used in different drive cycle schemes to simulate real system behavior. The analysis is accomplished with experimental verification, highlights the advantage of the new approach for evaluating storage capacity. Also, it gives the static and dynamic (time dependency) equations to show an accurate system representation as a ready-made (black box) models, which will be used to determine the overall system performance.

Peer-review under responsibility of the scientific committee of the 4th Annual CDT Conference in Energy Storage and Its Applications, Professor Andrew Cruden, 2019.

Keywords: Flywheel energy storage units; Energy recovery; Ready-made model; Storage capacity

1. Introduction

In electric vehicles (EVs) and hybrid electric vehicles (HEVs), RB can be used to restore kinetic energy. In RB, at the instant of braking, the electric motor connected to the flywheel works as a generator to convert rotational mechanical energy into electrical energy. The variable characteristic of the voltage generated from the generator/flywheel at braking is used to charge the storage unit [1,2]. This variable produced voltage depends

* Corresponding author at: School of Engineering, Cardiff University, CF243AA, UK.
E-mail addresses: AlamiliAM@cardiff.ac.uk, adnan.alaamili@uokufa.edu.iq (A. Alamili).

https://doi.org/10.1016/j.egyr.2020.02.026

Peer-review under responsibility of the scientific committee of the 4th Annual CDT Conference in Energy Storage and Its Applications, Professor Andrew Cruden, 2019.

on the flywheel's rotating inertia and on the capacity of both the generator and the storage unit, which can be identified experimentally [3]. Furthermore, mathematical models of dynamic systems are necessary for most fields of scientific research, and they can take many different structures, such as differential equations, state–space equations and transfer functions. The most widely used method for numerical demonstrations involves the development of mathematical equations based on the known physical laws that govern the system's attitude [4,5]. The disadvantages of this approach are that the resulting models are often complex and are not readily estimated by the available data due to identifiability problems. This issue makes it challenging to use this approach in applications such as control system design. If there is enough empirical or operational data, then the "identification system" can be used as an alternative to physical-based physical modeling. Also, this system is based on data that can be applied to virtually any system and generally provides relatively simple models that can well-describe system demeanor within a specific operating system. These models can be used in a "black box", which only represents the behavior of the input and output or other descriptive interiors such as state space equations, which can explain physically meaningful judgments [6,7].

This paper will display an introduction to the statics and dynamics equations of the various components represented as a ready-made (black box) models, which can be used in determining overall system performance. Accordingly, the general layout for the system is presented in both schematic and pictorial representations, for both motoring and braking (generating) configurations. Meanwhile, the flywheel that is connected to the brushless direct current (BLDC) motor in the test rig must provide continuous power for a time to charge the UC during the braking process. The goal is to achieve regulation of the generated voltage to make the system as efficient as possible. Based on the results, some conclusions are given for the effect of rotating inertia at a different rotating speed and braking response on energy recuperation at different stages in the RB system.

2. Characteristics of the flywheel energy storage unit

In the experimental works, the flywheel can be used as a mechanical energy storage system (ESS). Kinetic energy is stored as rotational energy. In the test rig, the designed flywheel, which is a mass with high inertia rotating about the axis of the motor, is directly coupled to the rotor shaft of the "BL58EE70W" BLDC motor to increase the rotational inertia and to reduce the effects of initial acceleration (i.e. mechanical shock). Furthermore, excess energy is stored in the electrostatic field of the electrochemical UC storage unit (Eaton 16.2 V 65F). The circuit also includes a DC–DC converter, which is used for voltage regulation. The following section will describe the integration of different approaches to analyzing the flywheel energy storage (FES) unit, including mathematical and experimental verification and simulation.

2.1. The design requirements of the spinning flywheel ESS

The transit results in dynamic loads typically increase the required engine power. In addition, intermittent duties cause additional engine design issues. In industry, flywheels are used to influence a variable load [8]. The principle of a flywheel drive is based on the idea that peak load (i.e. shock load) only affects useful work, while it is unimportant in the free-running mode. The advantage of the flywheel is that idle energy accumulates on the inertial mass, which is then consumed in the working part of the cycle [9]. The shape of the flywheel is essential, and it must be designed so that the materials carry the same stress all the time. When used to store energy, part of its power is continuously dissipated as friction and aerodynamic losses. The estimated energy density is significantly affected by the additional weight of the bearings, motor/generator, and the shaft [10]. The flywheel (i.e. solid cylinder) in the designed test rig, was manufactured with a radius (r_2) of 8.75 cm, and a mass of 2.3 kg, as illustrated in Fig. 1a. All these components are placed in a steel guard, which protects the operator from the danger of the flywheel breaking at high speed.

When the flywheel is accelerated up to the desired speed, its kinetic energy E_{Kfly} is converted to electricity, which is then fed back to the system by using the motor as a generator or using another engine connected throughout a coupler; as shown in Fig. 1b. This depends on the moment of mass inertia (J_{fly}) for accelerating/decelerating, and a square of its rotational speed (ω), as follows:

$$E_{Kfly} = \frac{1}{2} J_{fly} \omega^2 \tag{1}$$

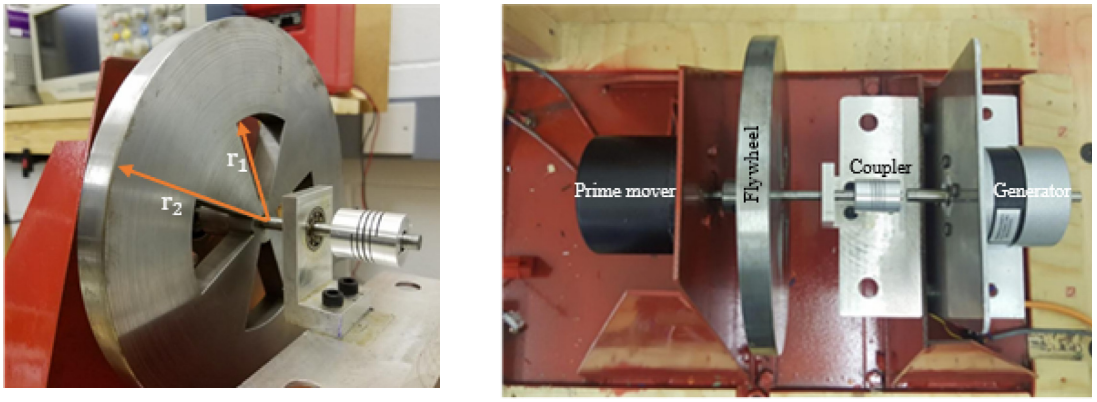

a- Designed flywheel b- Regenerative system

Fig. 1. Flywheel system photos.

The energy storage capability of the FES unit relies heavily on the analysis of Eq. (1), where, J_{fly} is the moment of inertia concerning the axis of rotation in (kg m^2), ω is the angular velocity of the rotating disc in (rad/s), and E_{Kfly} is the kinetic energy in (J). Moreover, the total torque applied to the flywheel T_{fly} is the electromotive torque T_{em} (N m) of the motor. In this case, its torque characteristic according to Newton's law of rotation, is expressed as follows:

$$T_{fly} = J_{fly}\,\alpha = J_{fly}\frac{d_\omega}{d_t} = T_{em} \tag{2}$$

where α (rad/s^2) is the spinning wheel angular acceleration.

By controlling the torque generated by the BLDC motor, the amount of energy transferred in and out of the flywheel can also be managed. Hence, charging and discharging of energy in the wheel is performed by dictating a positive and (or) negative torque command the BLDC controller.

For a solid disc flywheel of mass m in (kg) and radius r in (m), J_{fly} will be:

$$J_{fly} = \int r^2\,dm = \frac{1}{2}mr^2 \tag{3}$$

Eq. (3) indicates that a flywheel mass can be modeled as an active load connected to the rotor shaft of an electric machine. The rotational speed of the flywheel limits the stored kinetic energy. Hence, the energy accumulated (E_{acc}) of the moment of inertia applied at the speed change from ω_{max} to ω_{min} is given by [9] as in Eq. (4) as follows:

$$E_{acc} = \frac{1}{2}J_{fly}\left({\omega_{max}}^2 - {\omega_{min}}^2\right) = \frac{1}{2}J_{fly}\,{\omega_{max}}^2\left(1 - ({\omega_{min}}^2/{\omega_{max}}^2)\right) \tag{4}$$

Meanwhile, the energy density (E_d) (J/kg), often, only useful or usable energy is measured, while the inaccessible energy (such as remaining cluster energy) is ignored. For a flywheel, this can be defined as the ratio of energy stored to its mass. From Eqs. (1) and (3), the energy density can be represented as in Eq. (5) as:

$$E_d = \frac{1}{4}r^2\omega^2 \tag{5}$$

Moreover, to evaluate the rotational power, it is essential to convert the angular velocity (n) measured in rev/min to units of rad/s, as in Eq. (6) such that:

$$\omega(\text{rad/s}) = n(\text{rev/min})2\pi/60 \tag{6}$$

Furthermore, the time required for a flywheel to reach its nominal speed can be defined as:

$$t = 2\pi n/(60\,d\omega/dt) \tag{7}$$

Using the datasheet of the BL58EE70 W DC motor [11], at a nominal speed of 3300 rpm, the torque is 0.2 N m, and the time to reach this speed is 11.33 s, as follows:

From Eq. (3), $J_{fly} = \frac{1}{2}\ m(r_2{}^2 - \frac{1}{2}r_1{}^2) = 0.00655\ \text{kg m}^2$,

From Eq. (2), $\frac{d\omega}{dt} = \frac{T_{em}}{J_\omega} = 0.2/0.00655 = 30.5\ \text{m/s}^2$, and then, from Eq. (7),

$$t = \frac{2\pi n}{60\frac{d\omega}{dt}} = \frac{2\pi\ 3300}{60 * 30.5} = 11.33\ \text{s}$$

2.2. System under considerations

The overall system power flow in motoring and braking can be represented, as shown in Fig. 2.

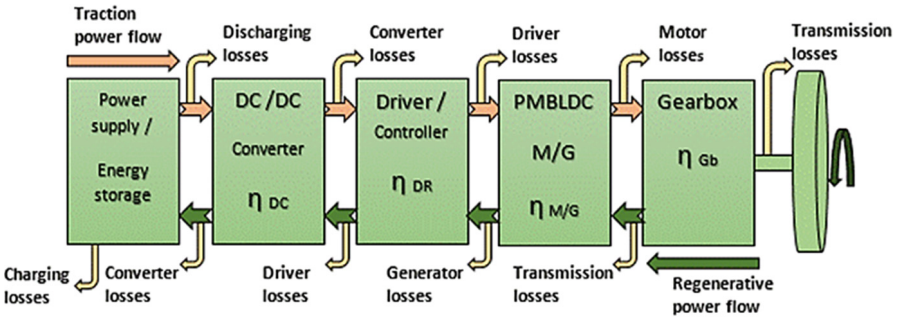

Fig. 2. System under consideration.

The electrical power (P_e) supplied to the BLDC motor is converted into mechanical power (P_m) by means of an addition to frictional power losses (P_{loss}), as $P_e = P_m + P_{loss}$. In the case of rotational mechanical motion, such as in EVs, the mechanical power (the rotational power (P_{rot})) is the product of torque T_{em} (N m) multiplied by angular velocity ω (rad/s), is expressed as in Eq. (8) as follows:

$$P_{rot} = T_{em}\omega = E_{back}I_a \tag{8}$$

where E_{back} is the generated induced back electromotive force (emf) (V), and I_a is the armature current (A). The rotational energy E_{rot} can be calculated as in Eq. (9) as;

$$E_{rot} = \int P_{rot}\ dt \tag{9}$$

Furthermore, in the designed test equipment, a semi-active configuration of excess energy recovery has been considered in the braking process that allows direct energy exchange between the UC and the bus. Also, the DC–DC boost converter controls the battery power flow, which engages the boosting battery voltage in motoring operation. This configuration was determined in the energy management system (EMS), which is out of this research aim.

2.3. Construction of the characteristic equation

In the designed test rig, the overall system response of BLDC motor (static and dynamic behaviors) which is connected directly with the flywheel, for both open-loop and closed-loop speed control can be represented in the flowchart as shown in Fig. 3a and b.

The extracted experimental data has been implemented from the open-loop test to estimate the system's behavior using characteristics equation.

The following calibration equations of every single element of the system have been extracted from Fig. 4:

• The voltage setting is an indication of the required motor speed (which provides calibration of the speed sensor used in the test rig). It is a linear function associated with compensation, which can be performed as follows:

$$y = 0.001x + 0.1047,\ R^2 = 0.9997 \tag{10}$$

• Drive input control voltage (potentiometer voltage) concerning set voltage, which is represented as in Eq. (11) as:

$$y = -0.0973x^2 + 1.3781x + 1.5659,\ R^2 = 1 \tag{11}$$

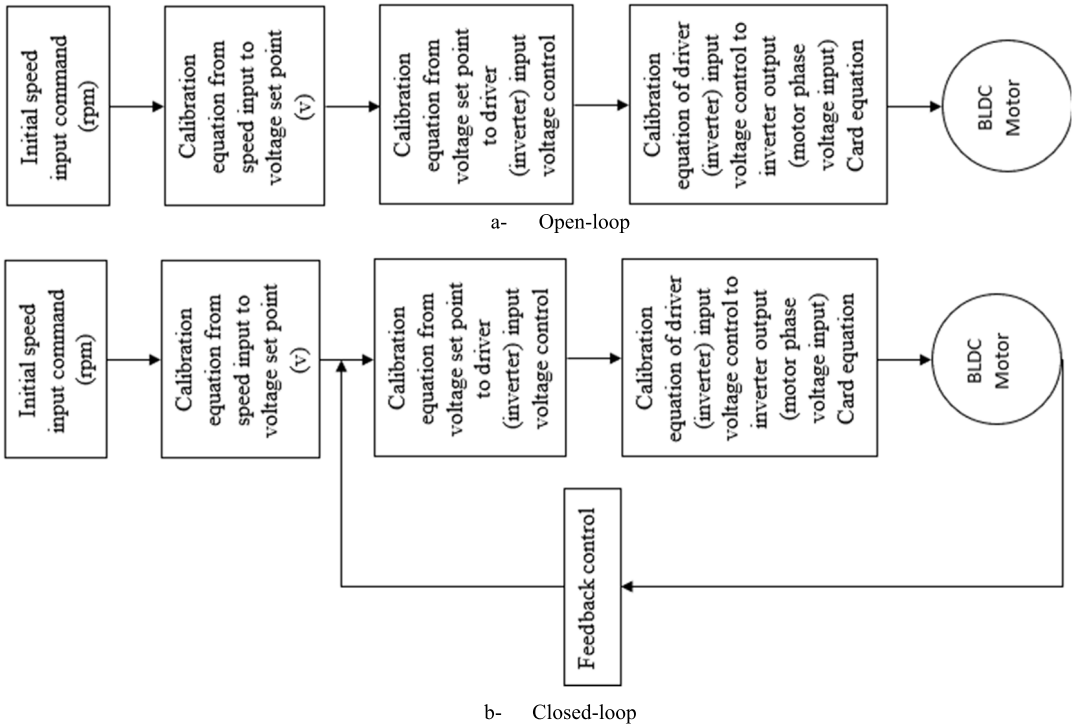

Fig. 3. BLDC motor speed control.

• Card characteristic equation, which is the output AC phase to ground voltage as a function of the input control voltage (inverter calibration equation), which is represented as in Eq. (12) as:

$$y = -0.4097x^2 + 4.5796x - 3.5866,\ R^2 = 0.997 \tag{12}$$

• Motor static equation, which is the speed as a function of its terminal AC voltage, which is taken as in Eq. (13) as:

$$y = 56.319e^{0.4421x},\ R^2 = 0.9966 \tag{13}$$

Furthermore, the dynamic response was derived from the motor speed-time graph to complete the overall motor modeling as in Fig. 5a. A fourth-order difference equation can be used to fit the curve trends. However, this research proposed a linearization method, where the graph is compared with a simulated first-order transfer function ($tf = 1/(5s + 1)$). Fig. 5b gives the compatibility and uses the system identification tool for comparison to get the best curve fitting.

While many strategies can be used for braking, the best accomplished is RB because some of the dissipated power is returned to the system and stored in the storage units. Primarily, its operation comes from the electricity that is generated when the motor works as a generator during descending of the vehicle speed due to the rotational energy stored in the flywheel. Fig. 6a shows the test motor stopping time at 3000 rpm speed with no load connected to its terminals (i.e. due to the moment of inertia alone). From this curve, the characteristic equation of the generator can be extracted, and the system is represented as:

$$y = 0.00008x^2 - 0.0299x + 2.9294,\ R^2 = 0.9995 \tag{14}$$

The no-load speed graph is compared to the second-order simulated transfer function to complete the general modeling of the generator, ($tf = 1/(0.9s^2 + 0.6s + 1)$), which gives the symmetry and is compared with the system identification tool to get the best curve fit; as shown in Fig. 6b.

These Eqs. (10)–(14) were used to create a closed-loop simulation in a "LabVIEW" environment to study system's behavior with the effect of rotational inertia on energy recovery, which can then be widely applied to any system being tested using the same procedure.

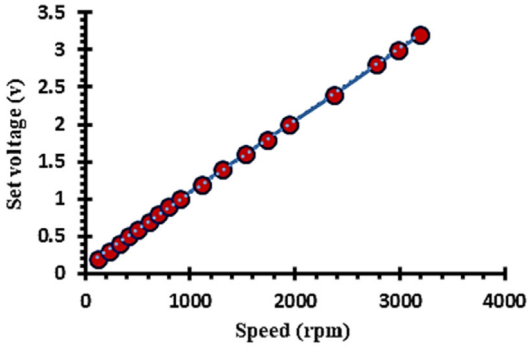

a- Set voltage as a function of the desired Speed

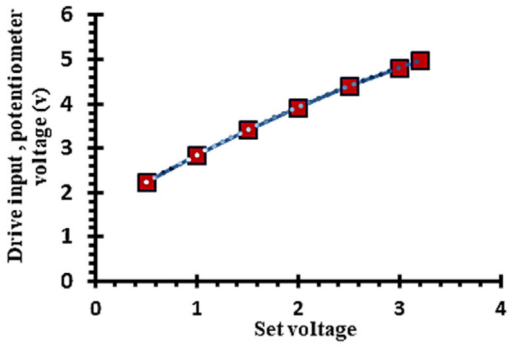

b- Drive input voltage as a function of the set voltage

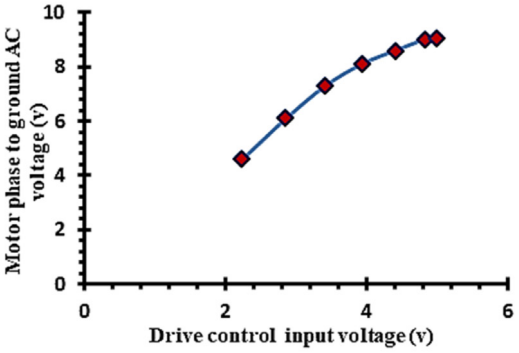

c- Motor phase to ground AC voltage concerning driving input voltage (card equation)

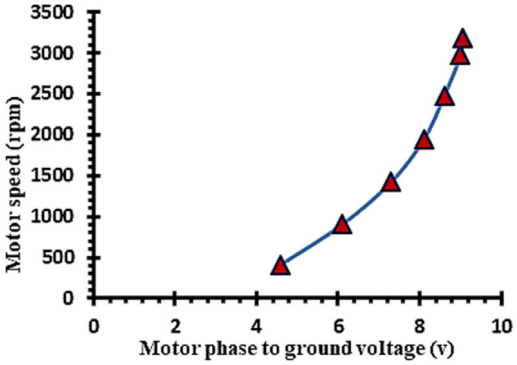

d- Motor speed as a function of motor phase to ground AC voltage (static relationship)

Fig. 4. Calibration equation of the test rig components.

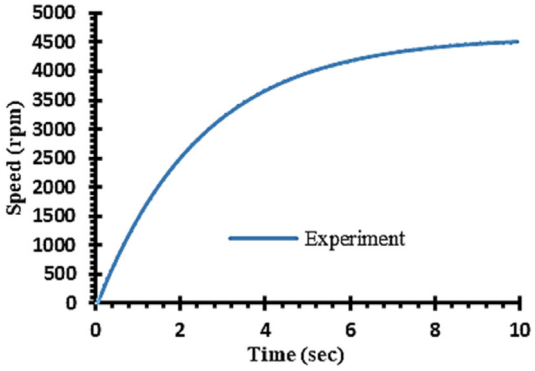

a- Experimental no-load response

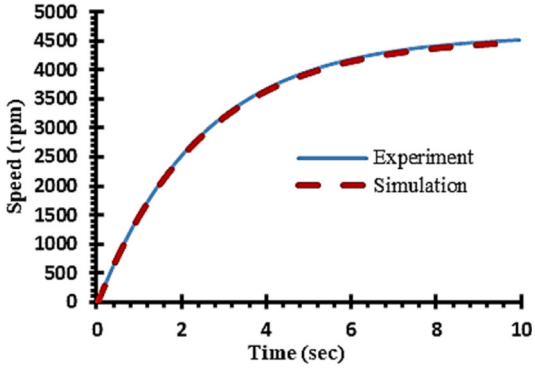

b- Simulated transfer function curve fitting

Fig. 5. BLDC motor dynamic response.

The overall system representation can be implemented as a flowchart, as shown in Fig. 7, which represents the motoring and generating operations with the energy stored in the UC storage unit.

3. Case study

In this study, the specifications of the test apparatus were used to build a closed-loop simulation that incorporates the system's element calibration Eqs. (10)–(14). The different aspects were used to investigate the impact of

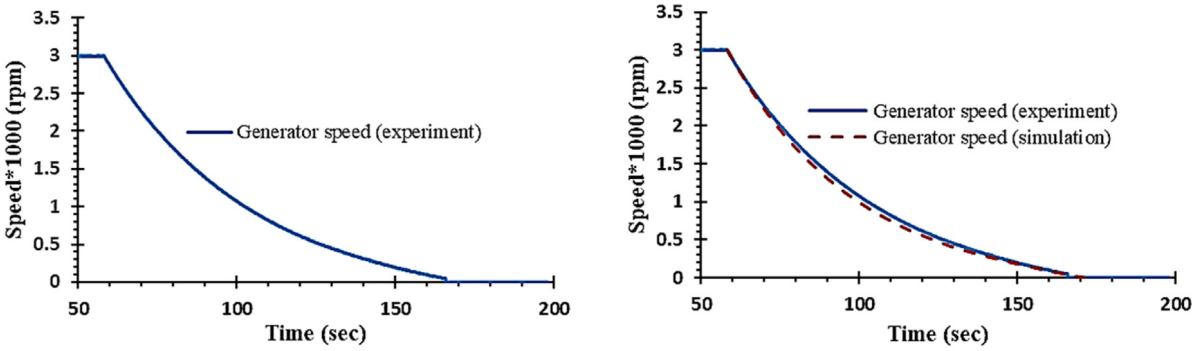

a- No load speed descending b- Simulated transfer function curve fitting

Fig. 6. BLDC generator (lumped with the flywheel) dynamic response.

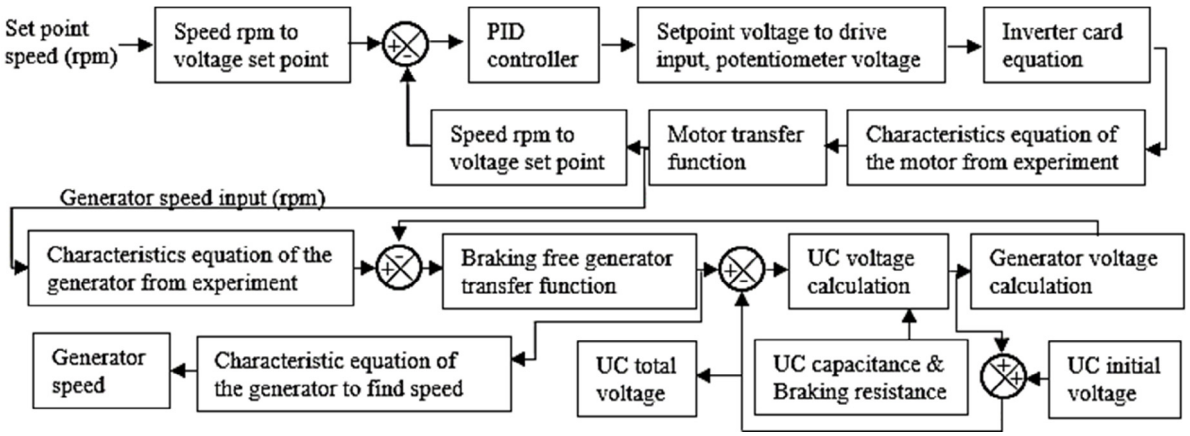

Fig. 7. Simulation flow chart.

rotational inertia. The stopping time, for example, depended on the speed of rotation and is also affected by the external load connected to the generator terminals. Studying the different region of operation will indicate the parameter of that load. Fig. 8 gives a spot point of the effect of the connected load on the stopping time;

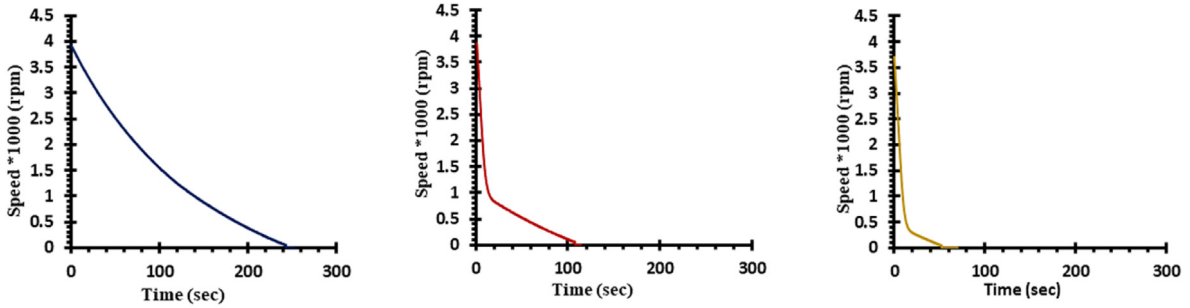

a- No-load b- 65F UC load c- 2000F UC load

Fig. 8. Variable load stopping time (braking) response at 4000 rpm speed.

Fig. 9b shows the area enclosed between the no-load and load curves. From this figure, it can be seen that as the area increases, the recovered energy increases, thus this affects the downtime. When comparing these curves, Fig. 9c indicates that there is no recaptured energy in the region where these two curves coincide.

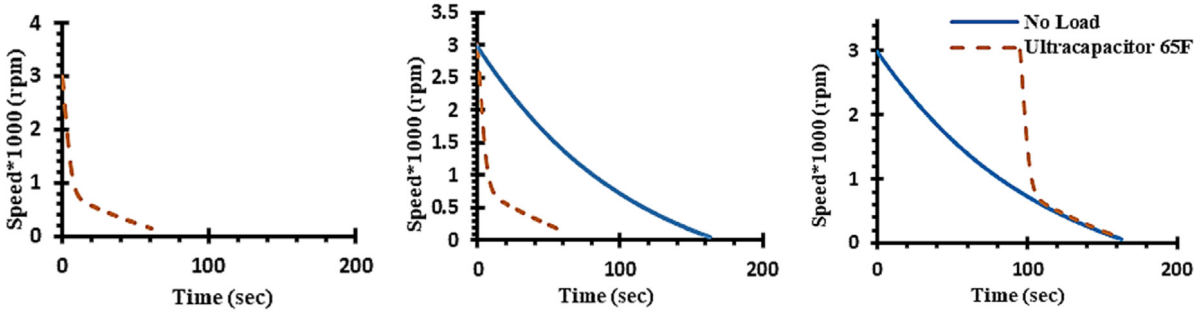

a- 65F UC load b- Compared with no-load c- Region of unrecovered energy

Fig. 9. Region of operation of 65F UC load at 3000 rpm.

The effect of rotational inertia on the voltage generated and, on the energy stored, is as shown as in Fig. 10b and c.

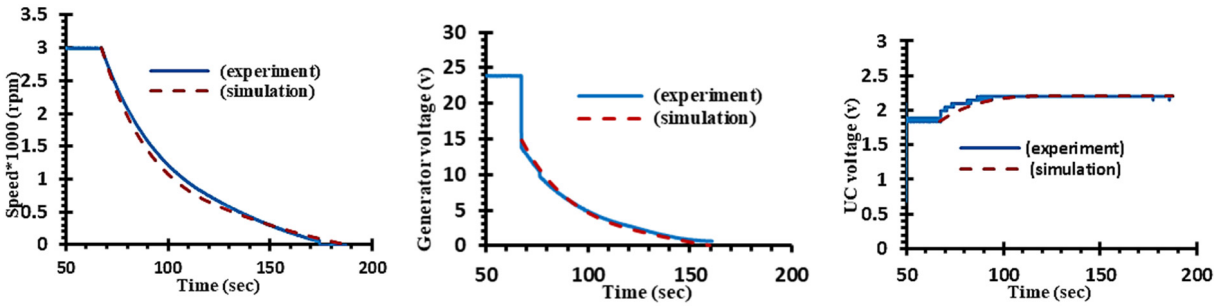

a- Generator speed b- Generator voltage c- UC voltage

Fig. 10. Rotational inertia effect on generated and stored energy.

Table 1 shows the voltage generated at 3000 rpm due to the flywheel's moment of inertia on the storage unit at different voltage stats and the time when there is no energy recapturing, which affects the overall system efficiency. The maximum recovered energy occurred when the UC is at minimum allowed voltage range, as shown in Table 1.

Table 1. UC state of charge at different charging times.

State	Speed UC stop charging (krpm)	UC initial voltage V_1 (V)	UC final voltage V_2 (V)	Change in voltage $\Delta v = V_2 - V_1$ (V)	Charging time t_{ch} (s)	Stopping time t_{tot} (s)	Wasted time $= t_{tot} - t_{ch}$ (s)	Energy $= 0.5*65*\Delta v\text{^}2$ (J)
1	0.45	0.1	1.28	1.18	29.4	85	55.6	45.253
2	0.597	1.31	2.33	1.02	27.6	96	68.4	33.813
3	0.8	2.38	3.2475	0.8675	25.12	104	78.88	24.4581
4	0.963	3.4	4.11	0.71	23.48	112	88.52	16.38325
5	1.127	4.37	4.925	0.555	21.8	120	98.2	10.011
6	1.32	5.337	5.795	0.458	20.097	127	106.903	6.81733
7	1.483	6.255	6.63	0.375	18.898	134	115.102	4.570
8	1.6	7.224	7.4788	0.25488	17.899	139	121.101	2.11132
9	1.77	8.192	8.396	0.204	16.601	144	127.399	1.35252
10	2.085	9.161	9.263	0.102	14	152	138	0.33813
11	2.309	11.5	11.52	0.02	12.5	159	146.5	0.013
12	2.462	12.5	12.51	0.01	11.3	170	158.7	0.00325

Figs. 11 and 12 show the regenerative activity related to the voltage state of the storage unit. The energy level and the charging time is maximum at the beginning, while it takes a long time to stop when the UC is fully charged.

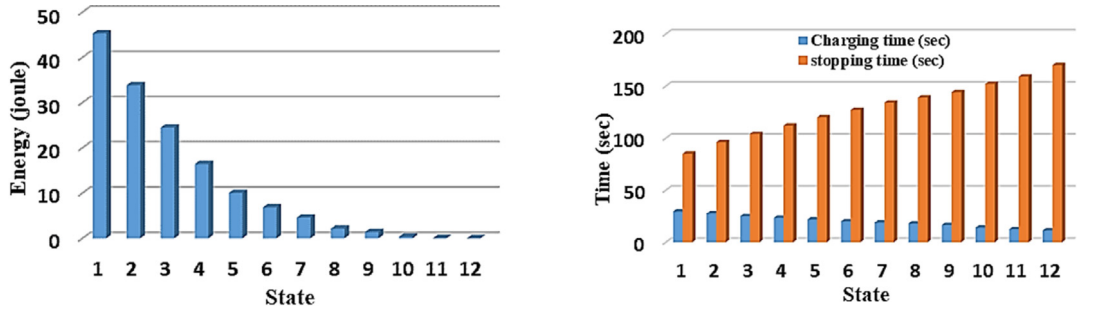

Fig. 11. Energy storage and time of operation at different state.

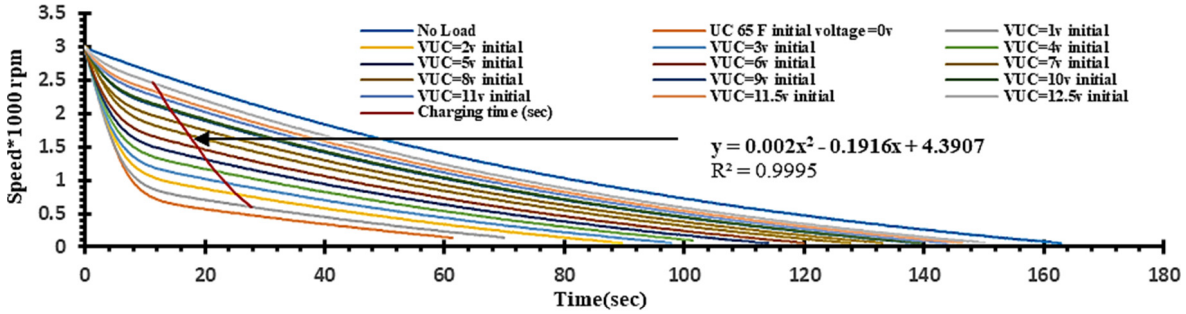

Fig. 12. The characteristic equation of the charging time of the RB process.

4. Conclusions

This study investigated a simulated FESs associated with the BLDC motor shaft. The flywheel inertia achieves adequate energy transfer in two-way power transmission during acceleration and deceleration. The proposed approach has been validated through a series of simulations and experimental tests. The impact of variations in the UC storage unit, voltage state and charge value, on the driving and RB characteristics (speeding and deceleration) highly depends on the kinetic energy stored in rotating inertia flywheels. Whereas the modeling and the analysis mainly depend on experimental results to represents the real system behavior, different stats are examined in this study to investigate the best representation of the designed system components in the laboratory environment and study the overall performance. The main contributions of this work are the development of a laboratory-based examination test rig to simulate the natural system that is based on energy recovery in the braking mechanism, and to study the effect of rotational inertia on energy recuperation in the RB process. The new approach to evaluate the static and dynamic equations of the lumped component and the evaluation of the transfer function shows an accurate system representation as a ready-made (black box) models.

Declaration of competing interest

The authors declare that they have no known competing financial interests or personal relationships that could have appeared to influence the work reported in this paper.

Acknowledgment

The corresponding author would like to thank the University of Kufa, Iraq, for sponsoring this research.

References

[1] Bolund B, Bernhoff H, Leijon M. Flywheel energy and power storage systems. Renew Sustain Energy Rev 2007;11(2):235–58. http://dx.doi.org/10.1016/j.rser.2005.01.004.

[2] Kim BH, Kwon OJ, Song JS, Cheon SH, Oh BS. The characteristics of regenerative energy for PEMFC hybrid system with additional generator. Int J Hydrog Energy 2014;39(19):10208–15. http://dx.doi.org/10.1016/j.ijhydene.2014.03.200.
[3] Alamili A, Xue Y, Anayi F. An experimental and analytical study of the ultra-capacitor storage unit used in regenerative braking systems. Energy Procedia 2019;159:376–81. http://dx.doi.org/10.1016/j.egypro.2018.12.073.
[4] Thoolen F. Development of an advanced high speed flywheel energy storage system. 1993, http://dx.doi.org/10.6100/IR406829.
[5] Hanselman DC. Brushless permanent magnet motor design. ISBN: 10:1-881855-15-5, 2006.
[6] Garnier H, Wang L. Advances in Industrial Control Series; Identification of Continuous-Time Models from Sampled Data. Springer-Verlag London Limited; ISBN: 9781848001602, 2008.
[7] Bohlin T. Advances in Industrial Control; Practical Grey-Box Process Identification Theory and Application. Springer-Verlag London Limited; ISBN: 9781846284021, 2006.
[8] Sebastián R, Peña Alzola R. Control and simulation of a flywheel energy storage for a wind diesel power system. Int J Electr Power Energy Syst 2015;64:1049–56. http://dx.doi.org/10.1016/j.ijepes.2014.08.017.
[9] Vodovozov V. Electric drive systems and operation. ISBN: 9788740301663, 2012.
[10] Clegg SJ. A review of regenerative braking systems. 1996, http://dx.doi.org/10.1016/S1366-5545(02)00012-1.
[11] BL58 EE-70 Watt. Premotec datasheet. 2001.